

ORIGINAL ARTICLE

Visualization of deep lung lymphatic network using radioliposomes

M.F. Botelho,^{a,*} J.J.P. de Lima,^a I.C. Dormehl,^b M. Fontes Baganha,^c C.M. Gomes,^a
A.C. Santos,^a J.N. Moreira,^d E. Kilian^b

^a*Instituto Biofísica/Biomatemática, IBILI, Faculdade de Medicina, Azinhaga de Santa Comba, Coimbra, Portugal*

^b*Institute for Life Sciences, Pretoria University, Pretoria, South Africa*

^c*Centro de Pneumologia da Universidade de Coimbra, Coimbra, Portugal*

^d*Centro de Neurociências e Biologia Celular de Coimbra, Faculdade de Farmácia, Coimbra, Portugal*

Received June 6, 2010; accepted November 11, 2010

KEYWORDS

Liposomes;
Lymphatic drainage;
Scintigraphy;
Pulmonary delivery;
In vivo studies

Abstract

Deep lymphatic drainage plays an important role in the lung, as it removes foreign materials laying on the airways surface, such as pathogenic microorganisms. This drainage is also associated with lung tumour dissemination route. Liposomes with a specially tailored membrane were used as foreign particles to be removed by the lung lymphatics. We aim to obtain images of deep lung lymphatics in baboons using liposomes encapsulating ^{99m}Tc-HMPAO, as aerosols. Axillary lymph nodes were visualized 30 min post-inhalation, becoming more evident 1 hour after, when abdominal aortic and inguinal lymph nodes were also observed. Late images added no additional information. ROI's and their time-activity curves were drawn to obtain biokinetic information. In conclusion, we can say that the proposed technique enables visualization of the deep lymphatic lung network and lymph nodes. This methodology may be an important tool for targeted lung delivery of cytotoxic drugs.

© 2010 Published by Elsevier España, S.L. on behalf of Sociedade Portuguesa de Pneumologia. All rights reserved.

PALAVRAS-CHAVE

Liposomas;
Drenagem linfática;
Cintigra a;
Libertação pulmonar controlada;
Estudos *in vivo*

Visualização da rede linfática profunda usando radioliposomas

Resumo

A drenagem linfática profunda desempenha um papel importante no pulmão, uma vez que remove materiais estranhos depositados sobre a superfície das vias respiratórias, tais como microrganismos patogénicos. Esta drenagem está igualmente associada às vias de disseminação tumoral. Liposomas com uma membrana especificamente desenhada foram usados para simular partículas estranhas a ser removidas pelos linfáticos pulmonares. Pretendem obter-se imagens dos linfáticos profundos em babuínos usando liposomas que encapsulam ^{99m}Tc-HMPAO sob a

*Corresponding author.

E-mail: lomena@bili.uc.pt (M.F. Botelho).

forma de aerossol. Observaram-se gânglios linfáticos axilares 30 min pós-inalação, que se tornaram mais evidentes 1 hora após, quando os gânglios abdominais e aórticos também se tornaram visíveis. Imagens tardias não acrescentaram informação relevante. Foram desenhadas ROI's (regiões de interesse), bem como as correspondentes curvas de actividade-tempo para obter informação acerca da biocinética. Em conclusão, pode dizer-se que a técnica proposta torna possível a visualização da rede linfática profunda do pulmão e os gânglios linfáticos. Esta metodologia poderá vir a ser importante na libertação pulmonar controlada de fármacos citotóxicos.

© 2010 Publicado por Elsevier España, S.L. em nome da Sociedade Portuguesa de Pneumologia. Todos os direitos reservados.

Introduction

The dense deep lymphatic network in the visceral pleural connective tissue, both in peribronchial and perivascular connective sheets, of all lung lobes, and in the juxta-alveolar regions plays a crucial role in removing foreign materials and in lung tumour dissemination.¹⁻⁵

Liposomes have been proposed as promising anti-tumoral drug carriers, due to their encapsulating ability.^{6,7} They are also suitable for imaging the deep lymphatic network, as they will act as foreign particles to be drained. They can be administered by several routes such as aerosols. Based upon the pathophysiology of *Bacillus tuberculosis* pulmonary infection, specific liposomes can be modulated. They can be made to mimic the membrane composition of the *Bacillus subtilis* spores (a respiratory tract saprophyte microorganism) in order to be captured by pulmonary lymphatics.^{8,9}

Materials and methods

Chemicals¹

Distearoylphosphatidylcholine (DSPC) was selected as the main phospholipid (transition temperature 56°C), enabling the production of stable liposomes in presence of biological fluids.^{6,7,10} Phosphatidylglycerol (PG) was chosen as a negatively charge phospholipid^{11,12} and glutamic acid (GA) acts as a residue, being present in the internal layer and in the dense outer layer.^{13,14} DSPC, PG, GA and GSH were obtained from Sigma (St. Louis, MO, USA), and Sephadex G-25 from Pharmacia (Uppsala, Sweden). For anaesthesia, Ketalar® (Parke Davis, Cape Town, S.A.) and Sagatal (Kyron Laboratories Pty. Ltd., Benrose, S.A.) were used. ^{99m}Tc was obtained from a commercial ⁹⁹Mo/^{99m}Tc generator (NECSA, South Africa). Exametazime (Ceretec™) was purchased

from G.E. Healthcare (UK). For labelling efficiency and radiochemical purity determination, strips of ITLC-SG (Gelman Sciences Inc., Ann Arbor, USA) and Whatman no. 1 paper were used.

Liposome preparation

The designed liposomal formulation is composed of DSPC:PG:GA, respectively 8:1:1, in molar ratio. The lipidic mixture with a 50 mg/mL concentration was dissolved in 2 mL of chloroform in a round-bottom flask. Then it was evaporated at room temperature, under reduced pressure and inert atmosphere, for 2 hours, to form a thin lipid film, which was dried overnight in vacuum.¹⁵ 100 mM reduced GSH in 0.9% saline was added to the films by energetic vortex mixing.¹⁶⁻¹⁹ The flask was placed in a water bath at 65°C for 10 min, to hydrate the lipidic film.

The produced multilamellar liposomes were then extruded at 70°C through two stacked polycarbonate filters (Nucleopore, CA, USA) of 100 nm pore size, mounted in a mini-extruder (LiposoFast™, Avestin, Canada) fitted with two 0.5 mL Hamilton syringes (Hamilton, NV, USA).²⁰⁻²² In order to obtain unilamellar liposomes, with small polydispersity index, they were passed through the filters 20 times.²³

To remove any remaining extravesicular GSH, the vesicle suspension (500 µL at a time) was eluted through a Sephadex G-25 gel molecular exclusion chromatography minicolumn at room temperature, plugged with a Durapore® membrane filter (Millipore, Ireland) of 0.45 µm pore size.²³⁻²⁶ The columns were washed with 0.9% saline, pH = 7.4, with a flow of ± 21 mL/h.^{15,22,27}

Labelling procedures

Liposome labelling was done according to Phillips et al.¹⁸ Ceretec® kits, containing 0.5 mg exametazime, 7.6 µg SnCl₂ and 4.5 mg NaCl were reconstituted with 740 MBq (20 mCi) of ^{99m}Tc pertechnetate in 1 mL of 0.9% NaCl solution, and incubated for 5 min.

Using a three step ITLC system, according to the manufacturer, the reconstituted kits were tested for contamination by free pertechnetate, reduced

¹ All chemicals and reagents not specified in the text were of analytical grade or equivalent.

hydrolysed ^{99m}Tc and hydrophilic ^{99m}Tc -exametazime complex, as well as for lipophilic ^{99m}Tc -exametazime.²⁸ Only kits with lipophilic ^{99m}Tc -exametazime > 80% were used for liposome labelling.

Approximately 3 mL of liposomal solution were mixed with 0.5 mL of ^{99m}Tc -exametazime. After 10 min of incubation, liposomes were separated of any free ^{99m}Tc using a sephadex G-25 column. Labelling efficiency of ^{99m}Tc -exametazime-liposomes was checked by ITLC-SG in 0.9 % saline. In this system, liposomes remain at the origin, while contaminants move with the solvent front.²⁸⁻³⁰

Liposome size and surface-charge measurements

Liposome surface charge was determined by laser Doppler velocimetry, using a Coulter Delsa 440 at 4 light incidence degrees: 34.7°, 26°, 17.4° and 8.7°. These data were used to calculate the electrophoretic mobility and zeta potential of the samples.

Vesicle size distribution was determined by dynamic light scattering or photon correlation spectroscopy analysis with a Coulter N4 Plus.^{31,32} The obtained diffusion coefficient was used to calculate the average hydrodynamic radius and, therefore, the mean diameter of the vesicles.^{32,33}

Stability studies

Liposome membrane permeability was evaluated in vitro along time by ITLC-SG with 0.9% saline. A decrease of labelling efficiency, i.e., loss of aqueous core content, can be used as an index of membrane integrity.

Liposome stability was evaluated by two methods: a) incubation at 37°C with: saline, human serum, human plasma and human serum albumin solution (4 mg/ mL), both fresh and after complement deactivation of blood fractions (56°C, 30 min), being saline and human serum albumin solution the controls;^{6,34} and b) ITLC-SG with saline, each 30 min, during 5.5 hours after a second sephadex G-25 gel molecular exclusion chromatography.

Effect of ultrasound (2.7 MHz frequency) on the integrity of the liposome membrane was also studied. Liposomes were evaluated before and after 3 min nebulization by microchromatography, using the previously described system.³⁵⁻³⁷

Aerosol production and administration

Aerosols were produced using an ultrasonic nebulizer (Heyer Ultraschall Verebler 69, Germany), generating US (ultrasound) of 2.7 MHz frequency².

The obtained heterodispersed aerosol was administered directly into a intratracheal tube inserted in the baboons' trachea (4 adult males, 25-27 kg), until about 2000 Kcounts/ min in the total field of view of the gamma camera were recorded (± 3 min). Animals were anaesthetised throughout the study. To induce anaesthesia Ketalar®

(10 mg/ Kg, i.m.) was used, immediately followed by a controlled infusion of Sagatal® (25-30 mg/ kg at 30 mL/ h, i.v.).

The urinary bladder of all animals was catheterized throughout the study, to drain the urine and enabling better pelvic image acquisition.

The effectively inhaled radioactivity dose (74 to 148 MBq) was determined using a calibrator (Capintec) and measuring the remaining labelled solution in the nebulizer after aerosolisation.

The protocol for the *in vivo* studies was approved by the Ethics Committee of the University of Pretoria, according to the guidelines of the national Code for Animal Use in Research, Education, Diagnosis and Testing of Drugs and Related Substances in South Africa³.

Biodistribution studies

Biodistribution studies were performed in four baboons (*Papio ursinus*) placed in dorsal *decubitus*, over the gamma camera (Siemens Orbiter, Siemens, Erlangen, Germany), following preliminary results obtained in *Sus scrofa*.³⁸ For dynamic acquisition (64 × 64 matrix, 1 frame/ min for 30 min) the collimator was placed under the thorax. The acquisition was synchronized with ^{99m}Tc -exametazime-liposome inhalation. A series of static images (128 × 128 matrix, 2 min/ frame) of thorax and pelvis was acquired at 30, 60, 90 and 120 min post-inhalation.

Indirect lymphoscintigraphy was done in one baboon, to confirm the inguinal lymph nodes localization. 18.5 MBq of ^{99m}Tc - Fe_2S_5 were injected into the first interdigital space of both feet to perform a 30 min dynamic acquisition (64 × 64 matrix, 1 frame/ min) of the pelvis. Immediately after a pelvic static image (128 × 128 matrix) was acquired, doing passive movements of both feet.

As a control, one baboon inhaled a ^{99m}Tc -exametazime aerosol. Dynamic acquisition followed the previously referred protocol, as well as the static images. These images were used as background for subtraction in the ^{99m}Tc -exametazime-liposome images.

ROIs were drawn over lung, heart, axillary lymph nodes, liver, kidney, and bladder dynamic images. In order to obtain biokinetic information, time-activity curves were plotted.

Statistical methods

Data are reported as mean \pm standard deviation. At-Student analysis was applied to the means, being the accepted probability for a significant statistical difference $p < .05$.

Results

The used methodology enabled production of unilamellar vesicles (mean diameter 50-100 nm) with a small polydispersity index (0.17, $n = 3$), and a surface charge of

² The water of the reservoir was cooled down to 5-6°C in order to minimize the effects of temperature increase produced by the US

³ In compliance with the European rules.

—45.8 mV (n = 3), confirmed by zeta potential and by photon correlation spectroscopy determination.

The labelling efficiency of the liposome formulation was tested by ascending instant thin layer microchromatography (ITLC-SG) with saline. The average labelling efficiency obtained for ^{99m}Tc -exametazime was $74.1 \pm 13.9\%$ (n = 12). The previously referred *in vitro* stability studies are shown in Figure 1A. Labelling efficiency of ^{99m}Tc -exametazime-liposomes was good, but the most important feature was that *in vitro* stability in the presence of human serum, human plasma and albumin solution was higher than in the presence of blood fraction.

The liposomal formulation was administered as an aerosol, and its labelling efficiency (after 3 min of US action) was not significantly different from the values determined pre- and post-US exposure. Study of liposomal aqueous core content loss, during 5.5 hours after the second ITLC, showed a good stability before and after ultrasonication (Fig. 1B).

Dynamic scintigraphic studies, both of ^{99m}Tc -exametazime and ^{99m}Tc -exametazime-liposomes aerosol inhalation, showed a good deposition in the lung, confirming that the produced liposomes reached the small airways and, hence, the alveolar surface.

Axillary lymph nodes were visualized 30 min post-inhalation. 1 hour post-inhalation they became more evident, and abdominal aortic and inguinal lymph nodes were also observed. Later images did not give additional information, although activity is observed in abdominal organs (Fig. 2).

The mean activity/pixel in each ROI, after background and decay correction, was used to plot regional time-activity curves, showing the radiotracer biokinetics variations in certain target areas during the study (Fig. 3). Total activity was measured in the lungs post-inhalation, as well as clearance rate ($t_{1/2} = 77$ min) (Fig. 3A). An increase of activity was simultaneously observed in axillary lymph nodes, reaching maximum activity values for axillary and inguinal nodes ± 60 min (Fig. 3B-D).

Promoting passive movement of the feet, after ^{99m}Tc - Re_2S_7 injection, the left inguinal node was visualized at 45 min, corresponding to the area visualized with ^{99m}Tc -exametazime-liposomes (Fig. 4A). In a control animal, ^{99m}Tc -exametazime biodistribution showed a lung fast clearance through alveolar-capillary permeability, which enabled a quick visualization of several organs (liver, gallbladder, spleen, kidneys and the ascending and transverse colon (Product datasheet, Ceretec[®], 2001). Nevertheless, lymph nodes were not evident; as abdominal activity masks the lymphatic abdominal chains (Fig. 4B).

Following MIRD⁴ rules and applying the absorbed fraction method to calculate the absorbed dose, the obtained values are similar to those used in conventional nuclear medicine routine studies, to evaluate alveolar-capillary permeability with aerosols.^{39,40}

Discussion

Pulmonary lymphatic network is crucial for alveolar and interstitial clearance, being responsible for removal of many substances, particles, dusts, or pathogenic agents. Preferential lymphatic drainage correlates with certain specific surface components, such as those present in microorganisms.

This paper describes the obtained results of the *in vivo* animal studies in normal baboons, using the referred formulation (^{99m}Tc -exametazime-liposomes), administered as an aerosol as a diagnostic imaging agent to visualize the deep lung lymphatic drainage.

This carrier could be used both for visualization and therapy, whether it encapsulates an imaging agent or a therapeutic drug, respectively. Since anionic compounds are quickly removed by the lymphatic network negatively charged small calibrated unilamellar liposomes were produced by extrusion through polycarbonate membranes of 100 nm pore size.⁴¹

Since ^{99m}Tc has 6 hours of half-life, labelling the liposome aqueous phase, after their formation, was done immediately prior to administration.^{7,11,18,23,24,34,42} Extrusion under moderate pressures was done, as liposome inhalation implied absence of organic solvents or detergents in the solution, to avoid possible allergic reactions.¹¹

In vivo stability of liposomes may change and be altered by complement aggression, depending on the lipidic composition of the membrane.¹⁰ To evaluate these disruptive effects, ^{99m}Tc -exametazime-liposomes stability was tested *in vitro*, by incubation with saline, fresh human: serum, plasma and serum albumin solution (4 mg/mL), as previously described. Results showed a statistically significant increase of labelling efficiency in presence of human serum and plasma for the studied formulation ($t = 3.2$; $p = .01$). This shows that biological fluids do not induce liposome aqueous content leakage. Stability to ultrasonication was determined analysing the labelling efficiency after 2.7 MHz US action. Results do not show statistically significant differences for labelling efficiencies pre- and post-US action, as previously mentioned by other authors.^{37,41-45}

Liposomal stability was also studied in terms of entrapped content loss (Fig. 1B), during 5.5 hours. Results showed a progressive increase of aqueous content loss, probably depending on the lipidic composition.

The inhaled thin liposomal aerosol duly reached the lung alveolar-capillary membrane. The vesicles could either be cleared by crossing the alveolar surface to lung interstitium after phagocytosis by alveolar macrophages, or directly through intercellular spaces or mucociliary escalator. Those, which crossed the interstitium, were eliminated by lymphatic drainage to the lymph nodes and subsequently to blood capillaries.⁴⁶⁻⁴⁸

Anatomically, pulmonary lymphatics can be grouped into two interconnected networks: the superficial pleural one, running in the connective tissue of the visceral pleura, and a deep intrapulmonary network forming the peribronchovascular lymphatics, located in the connective tissue sheets of the pulmonary bronchial and vascular trees. Several lymphatic capillaries can be seen in juxta-alveolar areas, in contiguity with the alveolar wall and separated from the alveolar lumen only by the alveolar epithelium and

⁴ Medical Internal Radiation Dose.

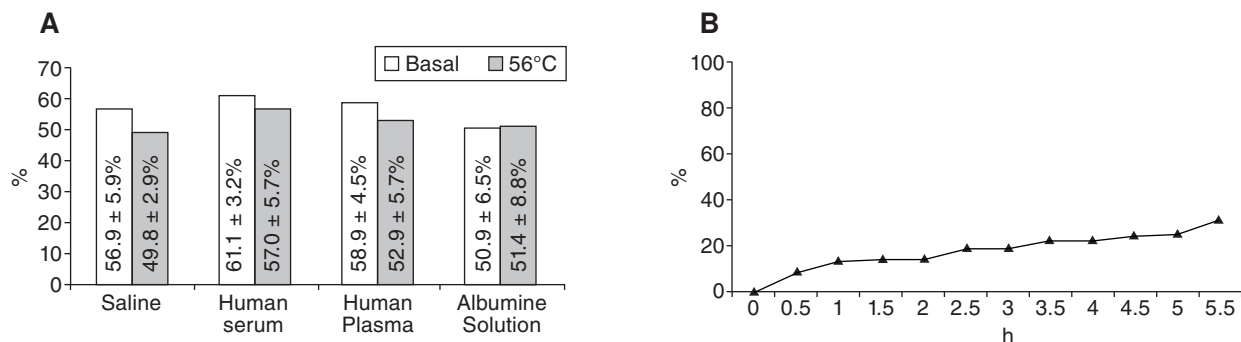


Figure 1 Stability of liposomes. A) Labelling efficiency (%) after incubation with different fluids (saline, human serum, human plasma, human serum albumin solution with a concentration of 4 mg/mL), before and after warming at 56°C for 30 min, in order to inactivate the complement of blood fractions. B) Temporal evaluation of the liposomes' aqueous core loss, using ascendant ITLC-SG with saline.

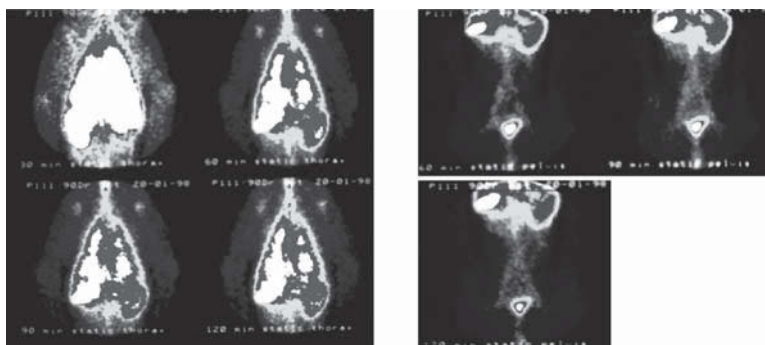


Figure 2 Image sequence obtained at 30, 60, 90 and 120 min after ^{99m}Tc-exametazime-liposome inhalation. Besides the high lung deposition, an high uptake by the axillary nodes should be noticed. In abdominal projections at 60, 90 and 120 min abdominal aortic and inguinal lymph nodes can be observed.

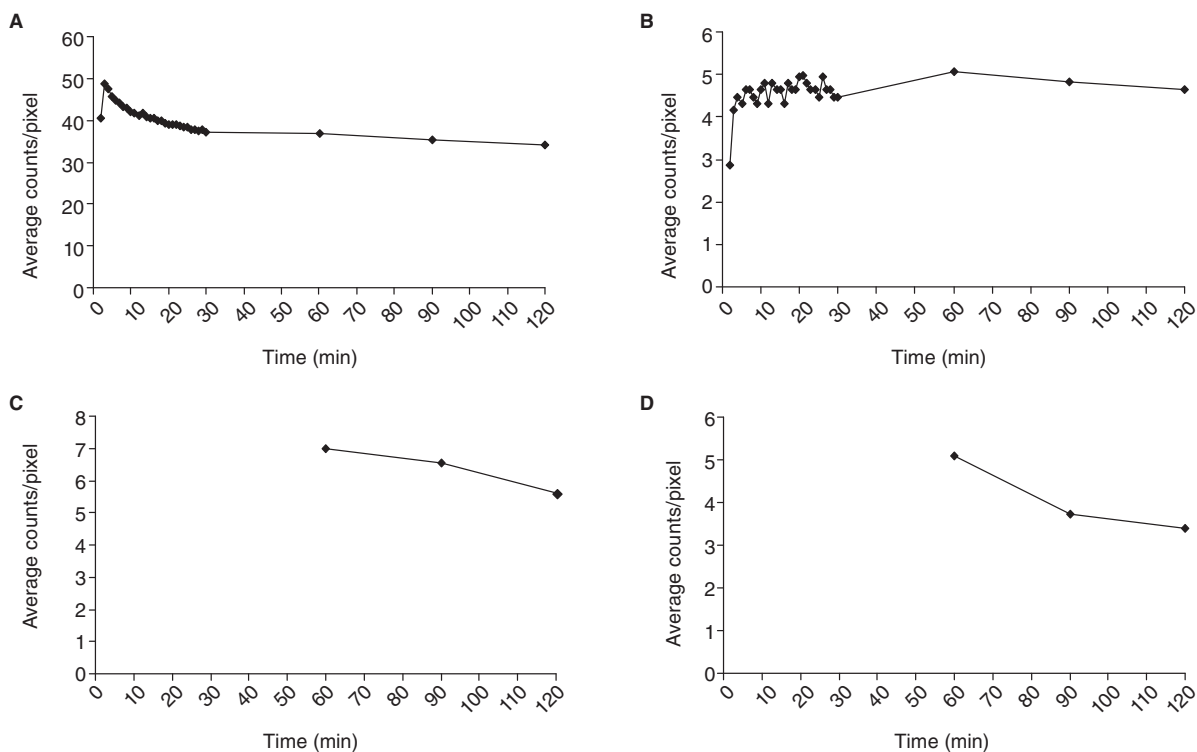


Figure 3 Time-activity curves representing the kinetics of the ^{99m}Tc-Exametazime-liposomes in the lungs (A), axillary (B), periaortic (C) and inguinal (D) nodes. Graphics C and D begin only at 60 min, since the collimator's dimension impairs to perform, simultaneously, a dynamic acquisition at thorax and abdominal levels.

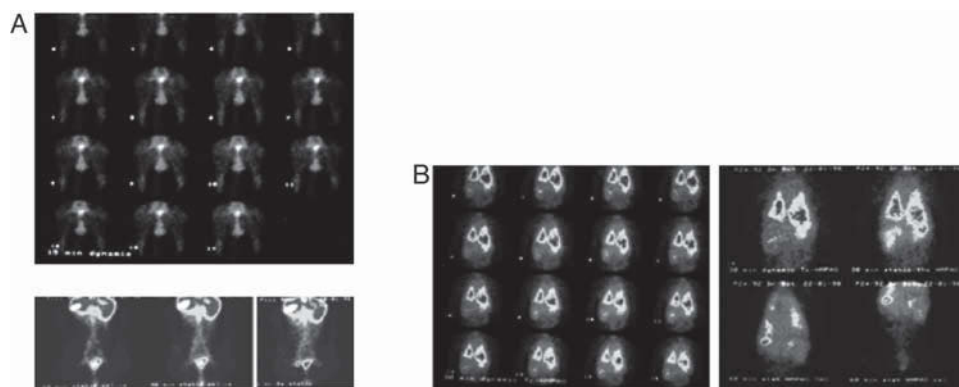


Figure 4 Animal controls. A) Dynamic image sequence of the indirect lymphoscintigraphy obtained during the first 30 min after interdigital feet ^{99m}Tc - Fe_2S_7 injection, as well as static images at 60, 90 and 120 min. The observed lymphatic abdominal drainage corresponds to the visualized areas with liposomes labelled with ^{99m}Tc -exametazime. B) ^{99m}Tc -exametazime biodistribution is a control and does not visualize the lymph nodes or lymphatic abdominal chains, only thoracic and abdominal activity uptake.

supporting connective tissue (usually very thin and richly vascularized). Pulmonary lymphatics can also be found in the loose connective tissue supporting more peripheral pleural cells and covering the pulmonary lobes, interalveolar septa and perivascular sheets.^{3-5,41,49}

The clearance mechanism also depends on physicochemical characteristics and particle size. Only submicronic sizes (< 50 nm \varnothing) can be deposited on the alveolar surface, being drained afterwards by the lymphatic system.⁵⁰ After reaching the alveolar surface, the ^{99m}Tc -exametazime-liposomes cross into the lymphatic capillaries of juxta-alveolar areas through intercellular gaps and are engulfed by alveolar macrophages, migrating then to the hilar lymph nodes.^{3-5,41,49,51} In our animal model, the rather high radioactive dose deposited in the lungs, did not help to identify these nodes. Nevertheless, the main lymphatic drainage route of the whole organ is linked to the mediastinal and abdominal periaortic lymph nodes, therefore their visualization in the images agrees with the anatomical data (Fig. 2).^{1-5,41,49,51} There is a fast infra-abdominal lymphatic drainage, post-inhalation, confirmed by indirect lymphoscintigraphy. This clearance can possibly explain distant metastasis of lung cancer appearing in unexpected sites.

Conclusions

Aerosols of specially tailored ^{99m}Tc -exametazime-liposomes proved to be an interesting approach to study deep lung lymphatic drainage. The physiological behaviour of these drug carriers, mimicking some properties of micro-organisms, allowed visualization of a descendant lymphatic pathway to the abdominal aortic chain nodes, confirmed by indirect lymphoscintigraphy. Images of these chains could give highly relevant information for staging lung tumours, as well as to evaluate other pathologies with important pulmonary lymphatic contribution. In addition, this methodology may play an important role in targeted lung delivery of other pharmaceuticals, e.g. cytotoxic drugs.

Taking into account the promising obtained results in the tested animal models, the production of a tracer, for

inhaled administration, providing information on the degree of pulmonary invasion and metastization through functional images, is in perspective.

Conflict of interest

Authors declare that they don't have any conflict of interest.

References

1. Leak LV, Ferrans VJ. In: Crystal RG, West JB, et al, editors. The Lung: Scientific Foundations. New York: Raven Press Ltd; 1997. p. 779-86.
2. Taylor AE, Barnard JW, Barman SA, Adkins WK. In: Crystal RG, West JB, et al., editors. The Lung: Scientific Foundations. New York: Raven Press Ltd; 1997. p. 1147-61.
3. Nagaishi C, Okada Y. In: Dereck JD, Navrozov M, editors. AP Fishman's Pulmonary disease and disorders, 2. London: McGraw-Hill Inc; 1980. p. 901-8.
4. Fishman AP. In: Dereck JD, Navrozov M, editors. AP Fishman's Pulmonary Disease and disorders, 2. London: McGraw-Hill Inc; 1980. p. 919-52.
5. Lauweryns JM, Baert JH. Alveolar clearance and the role of the pulmonary lymphatics. *Am Rev Respir Dis.* 1977;115:625-83.
6. Gregoriadis G, Florence AT. Liposomes and cancer therapy. *Cancer Cells.* 1991;4:1444-6.
7. Goins B, Klipper R, Rudolph AS, Phillips WT. Use of technetium-99m-liposomes in tumor imaging. *J Nucl Med.* 1994;35:1491-8.
8. Hanson RS, Peterson JA, Yousten AA. Unique biochemical events in bacterial sporulation. *Annu Rev Microbiol.* 1970;24:53-90.
9. Aronson AI, Fitz-James P. Structure and morphogenesis of the bacterial spore coat. *Bacteriol Rev.* 1976;40:360-402.
10. Finkelstein MC, Weissmann G. Enzyme replacement via liposomes. Variations in lipid composition determine liposomal integrity in biological fluids. *Biochim Biophys Acta.* 1979;587:202-16.
11. Gregoriadis G, Senior J. The phospholipid component of small unilamellar liposomes controls the rate of clearance

- of entrapped solutes from the circulation. FEBS Letters. 1980;119:43-6.
12. Zalustny MR, Noska MA, Gallagher PW. Properties of multilamellar liposomes containing $^{99m}\text{TcO}_4^-$: Effect of distearoylphosphatidylcholine to sphingomyelin ratio. J Nucl Med. 1986;13:269-76.
 13. Nayar R, Hope MJ, Cullis PR. Generation of large unilamellar vesicles from long-chain saturated phosphatidylcholines by extrusion techniques. Biochim Biophys Acta. 1989;986:200-6.
 14. Op der Kamp JAF, Røedai I, Van Deenen LLM. Phospholipid composition of *Bacillus subtilis*. J Bacteriol. 1969;99:98-303.
 15. Tyrrell DA, Heath TD, Colley CM, Ryman BE. New aspects of liposomes. Biochim Biophys Acta. 1976;457:259-302.
 16. Mauk MR, Gamble RC. Preparation of lipid vesicles containing high levels of entrapped radioactive cations. Anal Biochem. 1979;94:302-7.
 17. Osborne MP, Richardson VJ, Jeysingh K, Ryman BE. Radionuclide-labelled liposomes -A new lymph node imaging agent. Int J Nucl Med. 1979;6:75-83.
 18. Phillips WT, Rudolph AS, Goins B, Timmons JH, Klipper R, Blumhardt R. A simple method for producing technetium-99m-labeled liposome which is stable in vivo. Nucl Med Biol. 1992;19:539-47.
 19. Jacquier-Sarlier MR, Polla BS, Sosman DO. Oxido-reductive state: The major determinant for cellular retention of technetium-99m-HMPAO. J Nucl Med. 1996;37:1413-6.
 20. Goins B, Phillips WT, Klipper R. Blood-pool imaging using technetium-99m-labeled liposomes. J Nucl Med. 1996;37:1374-9.
 21. Awasthi VD, Goins B, Klipper R, Phillips WT. Dual radiolabeled liposomes: Biodistribution studies and localization of focal sites of infection in rats. Nucl Med Biol. 1998;25:155-60.
 22. MacDonald RC, MacDonald RI, Menco BPM, Takeshita K, Subbarao NK, Hu L-R. Small-volume extrusion apparatus for preparation of large unilamellar vesicles. Biochim Biophys Acta. 1991;1061:297-303.
 23. Hope MJ, Bally MB, Webb G, Cullis PR. Production of large unilamellar vesicles by a rapid extrusion procedure: Characterization of size distribution, trapped volume and ability to maintain a membrane potential. Biochim Biophys Acta. 1985;812:55-65.
 24. Olson F, Hunt CA, Szoka FC, Vail WJ, Papahadjopoulos D. Preparation of liposomes of defined size and distribution by extrusion through polycarbonate membranes. Biochim Biophys Acta. 1979;557:9-23.
 25. Huang C. Studies on phosphatidylcholine vesicles. Formation and physical characteristics. Biochemistry. 1969;8:344-51.
 26. Patel HM, Boodle KM, Vaughan-Jones R. Assessment of the potential uses of liposomes for lymphoscintigraphy and lymphatic drug delivery. Failure of ^{99m}Tc -technetium marker to represent intact liposomes in lymph nodes. Biochim Biophys Acta. 1984;801:76-86.
 27. Juliano RL, Stamp D. The effect of particle size and charge on the clearance rates of liposome and liposome encapsulation drugs. Biochem Biophys Res Commun. 1975;63:651-8.
 28. Brochure GE. Healthcare.
 29. McDougall IR, Dunnick JK, Goris ML, Kriss JP. In vivo distribution of vesicles loads with radiopharmaceuticals: A study of different routes of administration. J Nucl Med. 1975;16:488-91.
 30. Kasi LP, Lopez-Berestein G, Mehta K, Rosenblum M, Glenn HJ, Haynie TP, et al. Distribution and pharmacology of intravenous ^{99m}Tc -labeled multilamellar liposomes in rats and mice. Int J Nucl Med Biol. 1984;11:35-7.
 31. Saari SM, Vidgren MT, Koskinen MO, Turjanmaa VMH, Waldrep JC, Nieminen MN. Regional lung deposition and clearance of ^{99m}Tc -labeled beclomethasone-DLPC liposomes in mild and severe asthma. Chest. 1998;113:1573-9.
 32. Shurtenberger P, Hauser H. Characterization of the size distribution of unilamellar vesicles by gel filtration, quasi-elastic light scattering and electron microscopy. Biochim Biophys Acta. 1984;778:470-80.
 33. Pervucnik G, Shurtenberger P, Hauser H. Size analysis of biological membrane vesicles by gel filtration, dynamic light scattering and electron microscopy. Biochim Biophys Acta. 1985;821:169-73.
 34. Mayer LD, Hope MJ, Cullis PR. Vesicles of variable sizes produced by a rapid extrusion procedure. Biochim Biophys Acta. 1986;858:161-8.
 35. Hnatowich DJ, Clancy B. Investigations of a new, highly negative liposome with improved biodistribution for imaging. J Nucl Med. 1980;21:662-9.
 36. Taylor KMG, Taylor G, Kellaway IW, Stevens J. The stability of liposomes to nebulization. Int J Pharm. 1990;58:57-61.
 37. Leung KKM, Bridges PA, Taylor KMG. The stability of liposomes to ultrasonic nebulization. Int J Pharm. 1996;145:95-102.
 38. Botelho MF, Marques MA, Gomes C, Silva AM, Bairos V, Santos Rosa MA, et al. Nanoradioliposomes molecularly modulated to study the lung deep lymphatic drainage. Rev Port Pneumol. 2009;XV:261-93.
 39. Thomas S, Atkins H, McAfee J. Radiation absorbed dose from Tc-^{99m} diethylenetriamin pentaacetic acid (DTPA). J Nucl Med. 1984;25:503-5.
 40. International Commission of Radiation Protection Publication 30. New York; Pergamon Press; 1988.
 41. Parker JC. Transport and distribution of charged macromolecules in lung. Adv Microcirc. 1987;13:150-9.
 42. Goins B, Klipper R, Rudolph AS, Cliff RO, Blumhardt R, Phillips WT. Biodistribution and imaging studies of technetium-99m-labeled liposomes in rats with focal infection. J Nucl Med. 1993;34:2160-8.
 43. Caride VJ. Technical and biological considerations on the use of radiolabeled liposomes for diagnostic imaging. Nucl Med Biol. 1990;17:35-9.
 44. Goodrich RP, Handel TM, Baldeschwieler JD. Modification of lipid phase behavior with membrane-bound cryoprotectants. Biochim Biophys Acta. 1988;938:143-54.
 45. Mc Callion ONM, Taylor KMG, Thomas M, Taylor AJ. Nebulization of monodisperse latex sphere suspensions in air-jet and ultrasonic nebulizers. Int J Pharm. 1996;133:203-14.
 46. Corry D, Kulkarni P, Lipscomb MF. The migration of bronchoalveolar macrophages into hilar lymph nodes. Am J Pathol. 1984;115:321-8.
 47. Langenback EG, Bergofsky EH, Halpern JG, Foster WM. Supramicron-size particle clearance from alveoli: Route and kinetics. J Appl Physiol. 1990;69:1302-8.
 48. Myers MA, Thomas DA, Straub L, Soucy DW, Niven RW, Kaltenbach M, Hood CI, et al. Pulmonary effects of chronic exposure to liposome aerosols in mice. Exp Lung Res. 1991;17:687-705.
 49. Nagaiishi C, Okada Y. The pulmonary lymphatic system. In: Dereck JD, Navrozov M, editors. AP Fishman's pulmonary disease and disorders, 2. London: McGraw-Hill Inc; 1980. p. 901-8.
 50. Muir DCF. In: Crystal RG, West JB, Cherniack NS, Weibel ER, editors. The lung: scientific foundations. New York: Raven Press; 1991. p. 1839-43.
 51. Crystal RG. In: Crystal RG, West JB, Cherniack NS, Weibel ER, editors. The lung: scientific foundations. New York: Raven Press; 1991. p. 527-38.